LIDAR-DERIVED SITE INDEX IN THE U.S. PACIFIC NORTHWEST – CHALLENGES AND OPPORTUNITIES

Demetrios Gatziolis

USDA Forest Service, PNW Research Station, Forest Inventory and Analysis, Portland, Oregon USA – dgatziolis@fs.fed.us

KEY WORDS: LiDAR, Site Index, Forest Inventory, Pacific Northwest, Douglas-fir.

ABSTRACT:

Site Index (SI), a key inventory parameter, is traditionally estimated by using costly and laborious field assessments of tree height and age. The increasing availability of reliable information on stand initiation timing and extent of planted, even-aged stands maintained in digital databases suggests that information on the height of dominant trees suffices for assessing SI. Light Detection and Ranging (LiDAR) is a technology proven capable of providing reliable estimates of tree height even at the individual-tree level. A rigorous evaluation of LiDAR-enabled SI estimation performed on coniferous stands of the coastal U.S. Pacific Northwest indicates that where stand structure and topographic conditions support a high-fidelity assessment of ground elevation, accurate (R^2 = 0.88) estimates of SI should be anticipated. In more challenging conditions the accuracy of the estimates lessens substantially. A limited evaluation of spatial SI predictions indicates that the distribution of the index might not always conform to the expectations commonly held by forest managers and planners.

1. INTRODUCTION

Site index (SI) is the most commonly used indicator of site productivity (Hägglund, 1981), forms the basis for many forest management activities (Zeide and Zakrzewski, 1993), and it is an integral component of forest inventory systems (Hanson et al., 2002). It is calculated as a function of the height of dominant trees at some reference age, usually in even-aged stands (Monserud, 1984; MacFarlane et al., 2000). The formulation of the function can differ between species or eco-regions. Assessment of SI is typically performed at selected locations within the forest where estimates of tree height and age are obtained via standard forest field mensuration techniques. To avoid bias in SI estimates, it is essential that trees participating into its calculation, sometimes referred to as site trees, meet certain selection criteria (Nigh and Love, 1999), including dominant status, absence of injuries or growth suppression, and a preferred range of age.

Obtaining reliable estimates of individual tree height and age is a laborious and costly process often inhibited by visibility constrains, wood density that does not allow tree trunk boring to determine age, etc. Because of these limitations, SI estimates have traditionally been restricted to locations hosting inventory plots, and spatial predictions of SI have been rare. Recent efforts to assess the spatial distribution of SI have relied on relating multiple environmental variables in a geographic information system via regression tree analysis, geostatistics, and multiple regression (Iverson et al., 1997; Gustafson et al., 2003; McKenney and Pedlar, 2003). There has been speculation (Louw and Scholes, 2002), however, that the multiple-variable approach will be gradually replaced by superior, in terms of predictions accuracy, physiologically based simulation models such as 3-PG (Landsberg and Waring, 1997) or PROMOD (Battaglia et al., 1999). A recent implementation of the 3-PG spatial model in Oregon, USA, that used monthly averaged climatic data, estimates of soil attributes, and Forest Inventory and Analysis (FIA) data from thousands of plots in national forests to produce SI maps of Douglas-fir (*Pseudotsuga menziesii* (Mirb.) Franco) showed promising results (R^2 = 0.55), despite issues related to plot size, density and georeference precision (Swenson et al., 2005). The coarse resolution of the 3-PG model's prediction (1 km^2) in Oregon, or of comparable multivariate models implemented elsewhere, limits their utility to forest planning and decision making at the strategic level only. The often substantial SI variability within a stand or tactical management units remains unknown.

The parsimonious parameterization of standard SI models indicates that where even-aged is the preferred or common forest stand structure and stand age is known, information on the height of dominant trees is sufficient for obtaining local estimates on forest productivity and SI. Because spatial predictions of tree height and other forest inventory parameters are restricted by financial and logistical constraints (St-Onge et al., 2004), forest managers and inventory specialists have long been regarding remote sensing as perhaps the only feasible alternative to field measurements for obtaining spatial predictions that meet established accuracy standards over entire management units (Turner et al., 2004). Remote-sensing-derived estimates of tree height are typically obtained via the classic parallax method. Applied either on stereopairs of analog aerial photographs (Worley and Landis, 1954) or more recently (and more efficiently) on digital high-resolution imagery (Korpela, 2004) the method was found to produce unbiased tree height estimates only where a precise the ground-level elevation could be assessed correctly at, or near, the base of trees, a prerequisite rarely met in closed-forest canopies (St-Onge et al., 2004).

Unlike aerial photography and other forms of optical remote sensing, Light Detection and Ranging (LiDAR), sometimes referred as airborne laser scanning (ALS), is capable of penetrating the forest canopy, and hence is well suited to describing the vertical structure of forests. Owing to the capacity of small footprint laser pulses emitted from the airborne scanning instrument to propagate through small canopy openings and echo at ground level, LiDAR is also capable of assessing ground elevation (Kraus and Pfeifer, 1998). Small-footprint scanning data comprise a set of points, sometimes known as 'returns', accurately and precisely georeferenced in three dimensions (Baltsavias, 1999). Assuming adequate return density (> 4 points / m^2), processing of the point cloud data allows individual trees to be detected

(Brandtberg et al., 2003), and digital models of the vegetation canopy surface (CSM) and (bare-) ground surface (GSM) to be generated (Hodgson et al., 2003; Clark et al., 2004). Estimates of height for individual trees are obtained by subtracting from the CSM value, at selected locations believed to represent tree crown apexes, the corresponding, in two-dimensions, GSM value. Variants of this approached have yielded height estimates for individual trees that rivaled the accuracy of those acquired in the field (Hyyppä, 2000; Persson et al., 2002; Andersen et al., 2006).

Because the estimates of tree height depend on the fidelity of the LiDAR-derived forest canopy and bare-ground models, vegetation and topographical conditions that promote uncertainty, and perhaps bias, in model values became sources of error in tree height estimation. Choices of parameter values and assumptions embedded into the algorithms used in generating the models can also contribute uncertainty or bias (Kobler et al., 2007). Canopy models derived from LiDAR data tend to underestimate the true vegetation surface. The negative bias has been attributed to the laser pulse not always hitting the tree apex (Næsset and Økland, 2002) and having to penetrate the canopy surface before reflecting the first significant return (Hill et al., 2002). GSMs are generated under the assumption that enough pulses penetrate thoroughly through the stand profile to enable an accurate assessment of bare-ground elevation. Ackermann (1999) reported that 20 to 40 percent of pulses may reach the ground under dense forest canopies. Reutebuch et al. (2003) found that even in dense coniferous stands the density of ground returns enabled construction of a GSM with root-mean-square-error (RMSE) of only 0.31 m. Other studies have reported though that in increasingly complex vegetation, multiple-scattering reflection or absorption of the energy carried by a pulse reduces the number of ground returns or causes returns from understory vegetation or tree trunks to be erroneously labeled as representing the ground (Harding et al., 2001; Raber et al., 2002, Hodgson et al., 2003). In forest stands with complex profiles, GSM overestimation of at least 1.5 m is common (Hodgson et al., 2003; Clark et al., 2004) and bias should be expected to increase further with even moderate slopes (Kobler et al., 2007).

Although many studies have investigated the fidelity of LiDAR-derived estimates of tree height (Næsset, 1997; Popescu et al., 2002; Maltamo et al., 2004), very few were performed in dense forests or in terrain characterized by steep slopes (Clark et al., 2004). The paucity of studies were laser scanning is used for estimating tree heights in forests that are both dense and situated on steep slopes is likely due to the fact that, in such conditions, it is logistically and financially exceedingly difficult to obtain reliable field measurements of tree height necessary for evaluating the height estimates derived from LiDAR data. The challenge is further intensified where precise height estimates are needed over an area, a prerequisite for assessing inventory parameters with spatial support such as SI, instead of only at selected locations. The objectives of this study that address these challenges were a. to evaluate the fidelity of LiDAR-derived estimates of SI, and b. to investigate potential patterns in the spatial distribution of Site Index in the structurally complex temperate rainforest growing on the steep terrain of the coastal U.S. Pacific Northwest. The evaluation is based on rigorously calibrated field data obtained by using survey-grade equipment on plots established specifically for this study.

2. METHODS

2.1. Study area

The 9500-ha study area is on the coastal mountains of Lincoln County, in the State of Oregon, USA (Figure 1), and centered approximately at 44° 32'N, 123° 39'W. More than 90 percent of the area is temperate rainforest, with mean annual precipitation of 2005 mm. Forty seven percent of the forests are privately

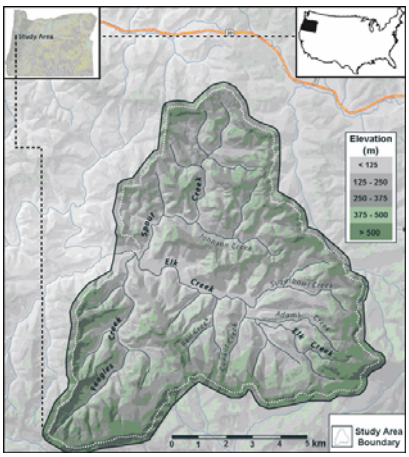

Figure 1. Study area

owned and under very intensive, timber-oriented management. 1550 ha are owned by the State of Oregon and 3850 ha are part of the Siuslaw National Forest where management has been limited to occasional non commercial thinnings, very few of which occurred after 1984. Prevalent species in the study area include Douglas-fir (*Pseudotsuga menziesii* (Mirb.) Franco), bigleaf maple (*Acer macrophyllum* Purgh), and red alder (*Alnus rubra* Bong.), with the hardwoods dominating buffer zones around the drainage network. Elevation ranges from 66 to 1123 m above sea level and terrain is characterized by steep slopes. Over the forest area the mean slope is 61 percent, and the 75th slope percentile is 84.

2.2. Field data

Forty five fixed-area plots of 15-m radius were established in the study area in summer 2005 stratified across classes of cover type (conifers, hardwoods, and mixed), tree size, and stand density. A three-member, veteran FIA crew visited each plot tallying all trees with diameter at breast height (DBH) exceeding 12.7 cm or of dominant or co-dominant status regardless of DBH. For each tree, the species and DBH was recorded, and the projection of its crown to the ground was delineated using distance and azimuth measurements from the tree base (Figure 2). Continuous feedback from the remaining crew members was used to guide a person operating a clinometer to on-ground locations that defined the shape of the crown being delineated. Estimates of tree height obtained via an electronic clinometer / distance finder were assigned a precision-class code reflecting the crew's confidence on the estimate. Two dominant trees in each plot were bored to determine age. Sketch maps depicting the presence, type, and height of understory vegetation were also produced.

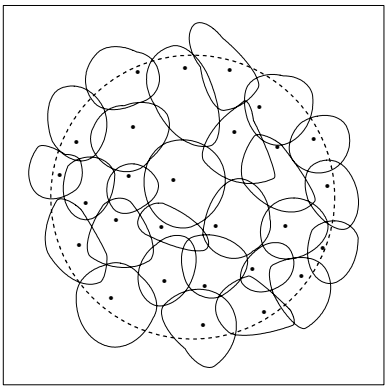

Figure 2. Field-delineated crowns of a plot and corresponding tree bases. The dashed line represents the plot boundary.

Management archives and stand maps from the Siuslaw National Forest and management plans or operation records kindly contributed by local tree farms were examined to determine the age of stands in nearly 75 percent of the forest land. After excluding all plots in uneven-aged or young (< 20 years) stands or where records suggested past stand improvement activities (fertilization, etc.), a set of 21 plots, all dominated by Douglas-fir, was selected and used in this study. The age of dominant trees ranged among the selected plots from 27 to 74 years. Plots comprising older and larger trees were in publicly owned stands.

The large percentage of height estimates assigned a low precision code in close-canopy stands confirmed skepticism that, in such conditions, traditional field mensuration techniques could not support the study's tree height precision requirements. To mitigate these limitations, an alternative, far more complex, approach was devised. It entailed a detailed survey of the bare ground and calibration of the tree crown apexes in each plot.

2.2.1. Plot registration and ground survey. For each plot a minimum of two locations was precisely referenced using a Real Time Kinematic (RTK) global positioning system instrument at leaf-off conditions. The instrument was set to record only when the expected, internally calculated, three-dimensional precision was better than 5 cm. Because the operation of the RTK instrument is limited to areas free from overstory vegetation, in 12 of the plots the closest two locations successfully recorded with the RTK were in canopy openings well outside the plot boundary. For those plots, transects connecting reference locations to corresponding plot centers were established and surveyed with a total station. For the remaining 9 plots, unobstructed, under canopy, lines of sight between the RTK reference locations and the plot centers supported direct plot georeferencing via the total station. Additional RTK reference locations and transects installed for 4 of the 12 plots revealed that the location error of the plot center ranged from 5.3 to 11.6 cm (mean 8.4 cm). Considering the difficult terrain and poor visibility conditions, the error level was deemed acceptable. With the total station positioned and oriented on the plot center, terrain inflection points were flagged over the plot area and a 5-m buffer around it. The flag density was higher in portions of the plots exhibiting variations in micro-topography. Across plots the density of flagged points had an average of 0.31 per square meter. Using Delaunay triangulation, the coordinates of flagged locations recorded with the total station were processed to generate a Triangulated Irregular Network (TIN) for each plot, and the TINs were then converted to 1-m rasters via cubic convolution. Five 10-m wide corridors transcending the boundaries of stands with contrasting stem densities and structure were also surveyed in late summer 2006, but with smaller point density. Canopy and ground models for the corridors were generated following the methodology used for the regular plots.

2.2.2. Calibration of tree apexes. Tree-apex calibration was performed by using 14 additional plots of custom size and shape installed either in short (< 3 m) vegetation or along the edge of Douglas-fir stands exposed by recent clearcuts. The leader stems of the trees were surveyed during windless days with the total station from three reference positions in the clearcut area previously surveyed with the RTK instrument. The methodology used is similar to the one detailed by Andersen et al. (2006). Trees with apex measurement RMSE exceeding 7.5 cm were eliminated from further consideration. A comparison of the coordinates of the surveyed apexes to the coordinates of co-located (within 1 m in two dimensions) highest LiDAR returns for 120 trees of various sizes and ages revealed an elevation bias of -0.58 m (Figure 3). The calibration procedure was repeated at leaf-off conditions with nearly identical results.

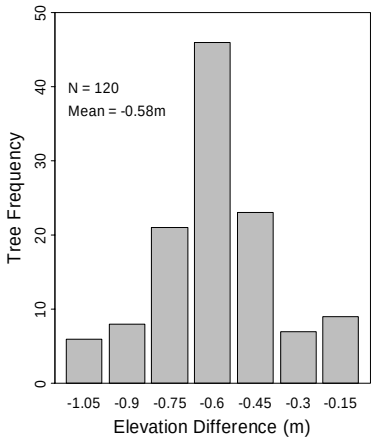

Figure 3. Histogram of discrepancies between surveyed and LiDAR-derived tree apex location at leaf-on conditions

2.2.3. Estimation of tree-height. To determine the heights of dominant and co-dominant trees in each plot, the field-delineated crowns were first overlaid with the return cloud. The elevation of the highest return within a crown was recorded and subsequently adjusted to account for the bias mentioned above. The calibrated tree height was then computed as the difference between the calibrated elevation of the highest return and the value of the GSM at the base of the tree. Calibrated heights for a total of 313 trees were computed.

2.3. LiDAR data

Laser scanning data were acquired at leaf-on conditions in July 2005 and leaf-off conditions in February 2006 using an aircraft-mounted Optech 3100 system from an average height of 1000 m above ground level. The LiDAR instrument operated on a 71 kHz laser repetition rate, captured a 20^{o} scan width (10^{o} from nadir) with adjacent flight line overlap of 50 percent, and yielded an average density of 9.81 returns per square meter for the leaf-on mission and 8.70 returns per square meter for the leaf-off mission. For both missions the spot spacing was 32 cm

with laser footprint diameter of 33 cm. Compared to horizontal, impermeable surfaces surveyed with the RTK, the laser returns sustained an RMSE of 2.6 cm during the leaf-on mission and 3.1 cm during the leaf-off mission. The scanning data delivered by the vendor had been processed with proprietary software to eliminate path reflectance points and to identify ground returns. The latter was enabled by an implementation of the adaptive TIN model (Axelsson, 2000). The raw (pre-filtered) data set for both missions was also obtained.

2.3.1. Canopy and ground models: For each plot, a 1-m canopy model was constructed by querying the returns cloud to determine the highest returns within the two-dimensional area occupied by each cell. Owing to the high return density and short pulse spacing, discontinuities in the canopy models were rare for both acquisitions and were observed only along the edge between adjacent crowns in plots with small canopy openings. GSMs were developed using the filtered returns classified as representing the ground via ordinary Kriging (Goovaerts, 1997) with a minimum of six nearest neighbors. Both canopy and ground surface models were co-registered to the GSMs generated from the survey data.

2.3.2. Tree identification and assessment. Individual trees were identified via the local maxima method (Wulder et al., 2000) using the LiDAR-derived canopy over the plot areas. After the elevation of GSM-identified tree apexes was bias-adjusted, the height of corresponding trees was computed as the difference between the tree apex elevation and the value of the co-located cell in the LiDAR-derived ground model. The local maxima method identified 294 trees. It was determined by visual examination of stem maps, delineated crowns, and the identified tree apexes that the tree list contained 26 errors of omission and 7 errors of commission.

2.4. Plot Site Index

The SI estimation for each plot followed the standard FIA protocol for Douglas-fir-dominated forest conditions. The protocol uses Equation 1, known as the King's (1966) formula, to compute estimates of SI for the five largest (in terms of DBH) or five tallest SI-eligible trees present within a 0.2 ac (809 m^2) area. The plot SI is then computed as the mean of the five estimates.

$$SI = \frac{\dfrac{25000 * (1.09757 + \dfrac{7.92236}{10^2} * A + \dfrac{1.97693}{10^3} * A^2)}{(\dfrac{3.2808 * A^2}{H - 14.764}) + \dfrac{9.5404}{10} - \dfrac{5.5818}{10^2} * A + \dfrac{7.3382}{10^3} * A^2} + 4.5}{3.2808} \quad (1)$$

where SI = King's SI in meters at reference age of 50 years
A = breast-height age
H = tree height in meters

Using classes of mean annual increment as reference, Equation 1 can be translated into a family of SI curves (Figure 4), commonly used to classify site productivity, instead of the actual SI values.

To investigate whether or to what extent tree selection affects the plot estimate, three SI versions were computed. The first (SI_D) was based on the trees with the largest, field-measured DBH. The second (SI_H) was based on the tallest trees identified in the field survey. The last version (SI_L) employed the tallest trees whose height was derived from the laser data. All versions used the stand age retrieved from the management records, adjusted for 6 years, the average time required for a tree to reach breast height from seed.

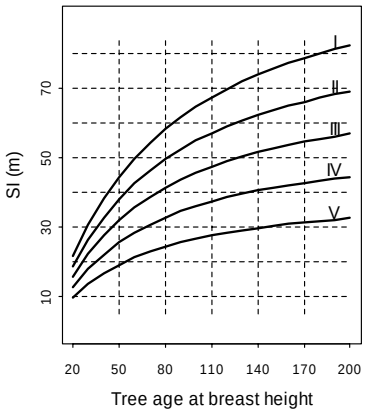

Figure 4. Douglas-fir Site Index classes for the coastal U.S. Pacific Northwest

2.4.1. Spatial predictions of SI. Investigations on the spatial continuity of SI focused on six areas, approximately 1 Km^2 each, where the stands present met the age and structure criteria for assessing SI. Given that reliable ground information, and therefore tree height, was available only for a single transect surveyed in each of these areas, the spatial investigations of SI were only exploratory in nature and employed omni- and directional variograms, along with an evaluation of potential trends (first-order spatial autocorrelation) in the predictions. The fidelity of SI maps produced was evaluated by visual, on-ground assessments performed while cruising the stands in the six focus areas.

3. Results

Tree age assessed by boring selected trunks was across plots, on average, 1.9 years (standard deviation 0.9) lower than the age expected from the stand history records. In the absence of cases showing the age determined by boring to exceed the age dictated by the records, and given that age underestimation for bigger trees where missed growth rings or failure to penetrate the trunk to its center is more common that in younger trees, there was no reason to doubt the accuracy of the stand age retrieved from management records.

Interesting insights into the interaction of dense coniferous vegetation and the laser pulses are obtained by subtracting the surveyed from the LiDAR-derived GSMs. For 10 of the 21 plots no macro-scale differences were observed between the surveyed ground surfaces and those computed from the leaf-on laser data. The paired discrepancies in cell values formed leptokurtic Gaussian distributions with means that ranged from -0.28 to -1.04 m. Nine of these 10 plots had little or no understory vegetation and the overstory had either been thinned in the past or contained regular canopy openings due to age progression. The 10^{th} plot (Figure 5b) had a very dense overstory but was located on mild (51 percent) slope. For another five plots, the discrepancies between surveyed and derived surface elevation were larger, up to -2.19 m, and the distribution of paired cell value differences was wider than in the previous group. In three of the five plots the distribution

was bimodal. All five plots had dense multi-layer understory vegetation with overstory exhibiting occasional openings. For the remaining six plots large scale discrepancies were observed between the surveyed and LiDAR-derived surfaces. The distribution of cell value differences had Gaussian form with means ranging from -4.97 to -11.02 m (Figure 5a). The plots in this group were either located on very steep slopes or had dense, completely closed canopies. Substituting the leaf-on laser data with the leaf-off version caused a slight reduction in the discrepancies between the surveyed and derived ground surfaces for the first two groups of plots with the mean differences in the first group now ranging from -0.18 to -0.84 m and in the second from -0.46 to -1.58 m. No improvement in ground-surface discrepancies was observed for the third group. The third was also the only group of plots where returns located above the surveyed ground were eliminated during data preprocessing, an observation pertaining to both acquisitions.

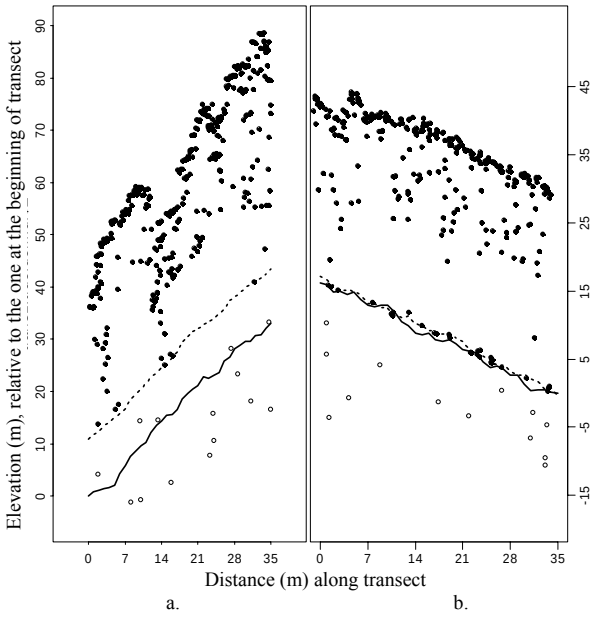

Figure 5. Plot profiles of 1 m depth depicting laser returns either maintained (dots) or filtered out (hollow circles) during data preprocessing, and surveyed (solid lines) and LiDAR-derived (dashed lines) ground surfaces.

In the process of overlaying the field-delineated tree crowns with the return cloud to evaluate the fidelity of individual tree identification procedure a pattern emerged that involved the relative location of tree apexes and bases. It was determined that for the majority of trees, the projection of the tree apex to the ground was downhill from the tree base, an indication that the trees were leaning systematically away from the slope. By considering that a tree was leaning if the horizontal distance between its apex and base exceeded 0.5 m, it was determined that 165 trees (53 percent) were leaning away from the slope, 50 trees (16 percent) were leaning in parallel to the contour lines, and 41 trees (13 percent) towards the slope. For the remaining 18 percent of the trees no appreciable leaning was observed. The intensity of the leaning was found to be positively correlated to slope and tree height, and negatively correlated to canopy closure, but the correlation was weak, with coefficients of 0.19, 0.16, and -0.17, respectively.

The option of selecting the trees with the largest DBH instead of the tallest ones was found to have little effect on the plot SI estimate. A t-test of the paired differences between SI values computed using the two alternatives methods for tree selection failed to reject the hypothesis that the SI estimates were equal ($p > 0.5$). Substituting, however, either one of the alternative field-data-assessed SI estimates in the test with their LiDAR-derived equivalent, rendered the test significant ($p<0.001$).

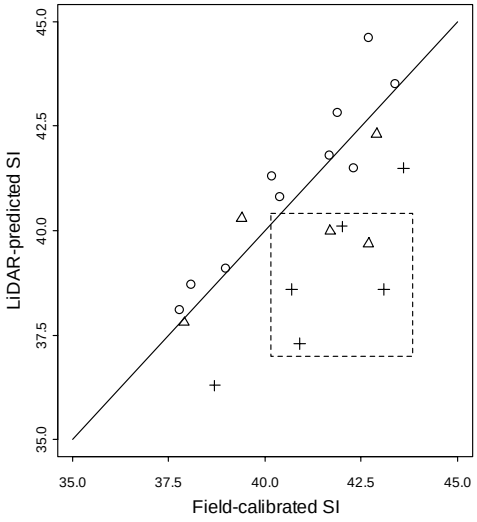

Figure 6. Plot Site Index values computed using the tallest trees surveyed in the field and their LiDAR-derived equivalent. Symbols indicate plot membership in classes of fidelity for the ground surface extracted from the laser data.

The causality behind the t-test findings becomes evident when examining the information in Figure 6, which compares the field calibrated and LiDAR-derived plot SI. Index values shown by circles in Figure 6 represent plots where the LiDAR-derived ground surfaces approximate the surveyed surfaces fairly well. In all but one of these plots, the predicted values exceeded the calibrated values, an indication that the tree height underestimation caused by the slight overestimation in ground elevation is somewhat overcompensated for by the trees leaning away from the slope. The values shown by crosses correspond to plots where the overestimation of ground elevation via LiDAR far exceeds the height overestimation due to leaning and results in index underestimation. With two exceptions, index values represented by triangles correspond to plots where elevation overestimation is somewhat balanced by tree height overestimation due to leaning. Note that 6 of the 11 plots in the last two groups (shown within a square in Figure 6) would be assigned an SI class of *II* when assessed via LiDAR and an SI class of *I* by using the calibrated field data. For the other 15 plots, the SI class assignment would not be affected by the method used to predict the index.

Regressions of the field-calibrated SI on the predicted values produced a low overall R^2 value of 0.42. The R^2 values pertaining to separate regressions computed using only the plot in each of the groups depicted in Figure 6 were substantially higher though, and for the group of plots established in medium density stands on moderate slopes, conditions that support assessment of ground elevation free from gross errors, it reached 0.88. Areas with conditions similar to those prevalent in the latter group of plot became the focus of investigations that evaluated the fidelity of spatial predictions of SI.

SI values predicted at 27-m intervals, the spacing equivalent to the size of field plots, were used to calculate omni- and directional variograms for each of the six, approximately 1km^2 areas where stand characteristics allowed computation of high-fidelity GSMs. A variogram quantifies how the values of a spatially distributed phenomenon change with distance. Typically, the value dissimilarity (semivariance) increases with distance until an asymptote (sill) is reached. The distance at which the sill is reached is known as the range of the variogram. Although there were notable differences in their form, all SI variograms computed for the six areas failed to reach a sill, thereby indicating the presence of low-order spatial autocorrelation(s), sometimes referred to as trend, affecting the predictions of SI. Of the many topographical covariates that were examined as a potential trend source (aspect, elevation, slope, wetness index, local ground curvature), only two were found to be significant at $\alpha = 0.05$; the distance to streams, which explained an average 9 percent of the SI variance across the six areas, and a composite variate computed as the natural logarithm of the slope cost distance away from streams, which explained 19 percent of the SI variance. Surprisingly enough, the percentage of SI variance explained increased to an average 31, almost a third of the total, when the variate was modified to be the natural logarithm of the absolute slope cost distance computed at 50 m from streams across contour lines. Variograms of the residuals of SI predictions (i.e. with the influence of the trend on the predicted SI values removed) regressed on the modified variate values did reach a sill, an indication that the remaining 69 percent of the SI variability is likely caused by genetic differences among the trees, soil characteristics, and variability in microclimate.

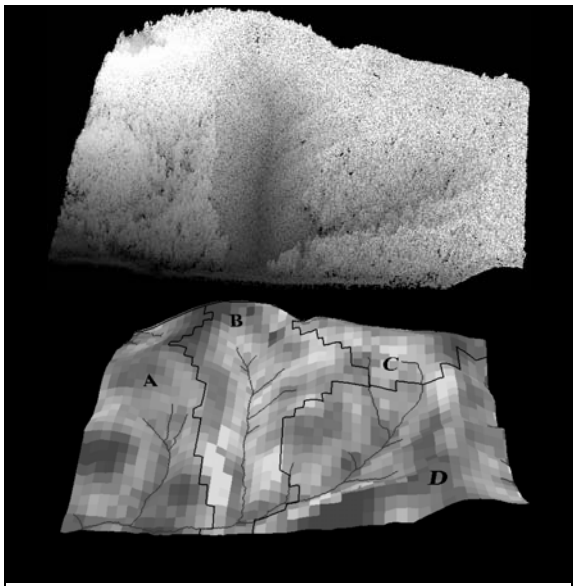

Management Unit	SI (st.dev) (m)	Mean Height (m) of SI Trees	Age (at breast height)	SI Cell Count
A	43.6 (2.66)	40.0	43	325
B	44.6 (3.48)	24.7	23	366
C	43.8 (3.43)	27.9	27	231
D	44.0 (2.51)	40.8	44	411

Figure 7. Top: Perspective view of the return cloud for a 1-km^2 area used in the evaluation of SI. Middle: Perspective view of SI predictions. Lighter tones indicate higher index values. The thick lines delineate management units; the thin lines represent the drainage network. Bottom: Descriptive statistics of SI predictions for each management unit.

Although only a third of the variability in the SI has been accounted by spatial variates, the absence of discontinuities across management unit boundaries (Figure 7) suggests that at a coarser scale, LiDAR-enabled assessment of SI yields robust results. In the area depicted in Figure 7, the mean predicted value for SI is practically the same for all four management units despite the stand age differences. The higher variability in the predicted values for units B and C is likely due to the slope of the SI curves being much steeper at smaller reference tree ages (Figure 4) than at older ages. A set amount of height variability for a group of adjacent younger trees would produce a higher SI variance than for a group of older trees.

4. Discussion

Evidence from the surveys of ground surface in this study and the analyses of laser data profiles in dense, coniferous canopies appear to contradict the commonly held belief that, given a high pulse density per unit area, enough pulses would penetrate the vegetation profile to allow detection of the forest floor. There appears to be a limit in canopy density, albeit difficult to quantify and likely different among forest cover types, beyond which the percentage of pulses that manage to penetrate the upper canopy layers exhibit substantially higher levels of path reflectance compared to the pulses penetrating less dense canopies. The implication of this phenomenon is that the already small amount of returns that are indeed reflected by the ground surface, are perceived as originating from much below. In such conditions, the density of legitimate ground returns is too small over extended areas to support the detection of ground surface.

Steep terrain introduces additional difficulties in ground detection. The algorithms used for the assessment of bare-ground utilize, sometimes directly, sometimes implicitly via simulation, slope thresholds to eliminate above ground returns. In 100 percent slopes or higher, the search radii associated with the slope thresholds that are used by the algorithms to quantify the spatial relationships between adjacent returns become so large that, inevitably, cause legitimate, above ground returns to be eliminated. Employing a more advanced algorithm for scan data filtering and ground assessment might have improved slightly the fidelity of tree height estimates and ultimately of the SI estimates but only for the plots located on milder slopes and with non-continuous canopies.

To minimize acquisition costs while maintaining high return density coverage, LiDAR instruments capable of increasingly higher pulse rates have been developed. Personal communication with LiDAR data vendors in the western U.S. has revealed that the 15-fold increase in pulse rates over the last few years has not been accompanied by an even near increase in the power the instrument outputs. Simply put, modern instruments emit more but weaker pulses. Studies that have successfully retrieved the ground surface in tropical (Clark et al., 2004) or in dense, coniferous forests (Reutebuch et al., 2003) have used pulse rates much lower than the one used in this study. Unless the per-pulse energy could be increased, in laser data acquisitions where unbiased retrieval of the ground surface is of essence, lower pulse rates might warrant consideration.

The decent correspondence (R^2 of 0.88) between field-calibrated and LiDAR-assessed SI in nearly half of the plots used in this study suggests, that in ecosystems and biomes with

topography and vegetation complexity less challenging than those in the coastal U.S. Pacific Northwest, high-fidelity index estimates should be expected. If the assumptions about absence of gross ground surface errors in the areas where spatial evaluations were attempted were valid, then useful information can be gleaned from such data at the spatial domain as well. The finding, for example, that a lag of 50 m from streams added to a spatial variate improves the percentage of variance in spatial SI predictions explained by that variate, challenges common beliefs held by local forest managers. Regulations limiting harvesting or other management operations to only outside 15 to 45 m buffers around streams and creeks are thought anecdotally to exclude from timber production the portion of the land with the highest growth capacity. This study hints that this in not the case. Perhaps excessive soil moisture near the drainage network early in the growing season may actually shift the most productive land at some distance uphill. The limited influence topography is found to exert on the values of the index could relate to the limited range of index classes present within the study area and the relatively small extent of the six areas evaluated. Upcoming LiDAR acquisitions over Douglas-fir stands growing on shallow soils and higher elevation might enable a more precise quantification of topography's influence on SI.

The applicability of the methodology used in the study to predict SI is limited to stands with even-aged, usually planted overstory and where detailed stand initiation and management records are available. It is also limited to species that maintain substantial, and hence LiDAR-discernible, height growth until older age classes. The study also indicates that because of substantial local variability in the height of dominant trees even within short distances, it is important that SI estimates be based on an adequate sample of trees.

5. Conclusion

The ability of LiDAR to penetrate stand profiles renders it a useful technology for quantifying the vertical dimension of forests and for assessing key inventory parameters such as SI. As this study has demonstrated, however, in dense forests with continuous, closed canopies growing on steep terrain, laser pulses often fail to penetrate the stands and to adequately sample the ground. Substantial errors in the assessment of ground elevation propagate through the computation of tree height and introduce bias in the predicted SI values. Additional, albeit smaller, bias is introduced by the underestimation of tree apex elevation and tree leaning. A better understanding of the mechanisms governing the interaction of laser pulses and dense vegetation could help predict the conditions where tree height and SI estimates might exhibit bias or increased levels of uncertainty. Extending the study area to include forest lands with lower SI index classes may allow detection and quantification of topographical gradients influencing the values of the index.

References from Journals:

Ackermann, F. 1999. Airborne laser scanning – present status and future expectations. *Photogramm. Rem. Sens.* 54:64-67.

Andersen, H.E., S.E. Reutebuch, and R.J. McGaughey. 2006. Rigorous assessment of tree height measurements obtained using airborne lidar and conventional field methods. *Can. J. Rem Sens.* 32(5):355-366.

Axelsson, P. 2000. DEM generation from laser scanner data using adaptive TIN models. *International Archives of Photogramm. Remote Sens.* 35(B3), Turkey.

Baltsavias, E.P. 1999. A comparison of between photogrammetry and laser scanning. *Photogramm. Remote Sens.* 54: 83–94.

Battaglia, M., P.J. Sands, and S.G. Candy. 1999. Hybrid growth model to predict height and volume growth in your Eucalyptus globulus plantations. *For. Ecol. Manage.* 120:193-201.

Brandtberg, T., T.A. Warner, R.E. Landenberger, and J.B. McGraw. 2003. Detection and analysis of individual leaf-off tree crowns in small footprint, high sampling density lidar data from the eastern deciduous forest in North America. *Rem. Sens. Envir.* 85(3)290-303.

Clark, M.L, D.B. Clark, and D.A. Roberts. 2004. Small-footprint lidar estimation of sub-canopy elevation and tree height in a tropical rain forest landscape. *Rem. Sens. Envir.* 91:68-89.

Gustafson, E.J., S.M. Lietz, and J.L. Wright. 2003. Predicting the spatial distribution of aspen growth potential in the Upper Great Lakes region. *For. Sci.* 49:499-508.

Hägglund, B. 1981. Evaluation of forest site productivity. *Forestry Abstracts*, 42:515–527.

Harding, D.J., M.A. Lefsky, G.G. Parker, and J.B. Blair. 2001. Laser altimeter canopy height profiles: Methods and validation for closed-canopy, broadleaf forests. *Rem. Sens. Envir.* 76:283-297.

Hill, R.A., D.L.A. Gaveau, and M. Spendlove. 2002. Accuracy issues in the assessment of deciduous woodland canopy height by airborne laser scanning: a case study. In *Proc. ForestSAT 2002 Conference, Edinburgh, UK*, August 5-9, 2002. Forestry Commission England and Forestry Commission Scotland, Edinburgh, UK.

Hodgson, M.E., J.R. Jensen, L. Schmidt, S. Schill, and B. Davis. 2003. An evaluation of LIDAR- and IFSAR-derived digital elevation models in leaf-on conditions with USGS Level 1 and Level 2 DEMs. *Rem. Sens. Envir.* 84:295-308.

Hyyppä, J., U. Pyysalo, H, Hyyppä, and A. Samberg. 2000. Elevation accuracy of laser scanning-derived digital terrain and target models in forest environment. In *Proc. EARSel-SIG-Workshop on LIDAR*, June 16-17, 2000, Dresden, Germany, pp. 139-147.

Iverson, L.R., M.E. Dale, C.T. Scott, and A. Prasad. 1997. A GIS-derived integrated moisture index to predict forest composition and productivity of Ohio forests (U.S.A.). *Landsc. Ecol.* 12:331-348.

Kobler, A., N. Pfeifer, P. Ogrinc, L. Todorovski, K. Oštir, and S. Džeroski. 2007. Repetitive interpolation: A robust algorithm for DTM generation from Aerial Laser Scanner Data in forested terrain. *Rem. Sens. Envir.* 109:9-23.

Kraus, K., and N. Pfeifer. 1998. Determination of terrain models in wooded areas with airborne laser scanner data. *Photogramm. Remote Sens.* 53:193-203.

Landsberg, J.J. and R.H. Waring. 1997. A generalized model of forest productivity using simplified concepts of radiation-use efficiency, carbon balance and partitioning. *For. Ecol. Manage.* 95:209-228.

Louw, J.H., and M. Scholes. 2002. Forest site classification and evaluation: a South African perspective. *For. Ecol. Manage.* 171:153-168.

MacFarlane, D.W., E.J. Green, and H.E. Burkhart. 2000. Population density influences assessment and application of site index. *Can. J. For. Res.* 30:1472-1475.

McKenney, D.W, and J.H. Pedlar. 2003. Spatial models of site index based on climate and soil properties for two boreal tree species in Ontario, Canada. *For. Ecol. Manage.* 175:497-507.

Maltamo, M., K. Mustonen, J. Hyyppa, J. Pitkanen, and X. Yu. 2004. The accuracy of estimating individual tree variables with airborne laser scanning in a boreal nature reserve. *Can. J. For. Res.* 34:1491-1801.

Monserud, R.A. 1984. Height growth and site index curves for inland Douglas-fir based on stem analysis data and forest habitat type. *For. Sci.* 30: 943–965.

Næsset, E. 1997. Determination of mean tree height of forest stands using an airborne laser scanner data. *Photogramm. Remote Sens.* 52: 49–56.

Næsset, E., and T. Økland. 2002. Estimating tree height and tree crown properties using airborne scanning laser in a boreal nature reserve. *Rem. Sens. Envir.* 79:105-115.

Nigh, G.D., and B.A. Love. 1999. How well can we select undamaged site trees for estimating site index? *Can. J. For. Res.* 29:1989-1992.

Persson, A., J. Holmgren, and U. Söderman. 2002. Detecting and measuring individual trees using an airborne laser scanner. Photogramm. *Eng. Rem. Sens.* 68(9): 925-932.

Popescu, S.C., Wynne, R.H., and Nelson, R.F. 2002. Estimating plot-level tree heights with lidar: local filtering with a canopyheight based variable window size. *Comput. Electron. Agric.* 37:71–95.

Raber, G.T., J.R. Jensen, S.R. Schill, and L. Schuckman. 2002. Creation of digital terrain models using an adaptive lidar vegetation point removal process. *Photogramm. Eng. Rem. Sens.* 68(12):1307-1315.

Reutebuch, S.E., R.J. McGaughey, H.E. Andersen, and W.W. Carson. 2003. Accuracy of a high-resolution lidar terrain model under a conifer forest canopy. *Can. J. Rem. Sens.* 29(5)527-535.

St-Onge, B., J. Jumelet, M. Cobello, and C. Véga. 2004. Measuring individual tree height using a combination of stereophotogrammetry and lidar. *Can. J. For. Res.* 34:2122-2130.

Swenson, J.J., R.H. Waring, W. Fan, and N. Coops. 2005. Predicting site index with physiologically based growth model across Oregon, USA. *Can. J. For. Res.* 35(7):1697-1707.

Turner, D.P., S.V. Ollinger, and J.S. Kimball. 2004. Integrating remote sensing and ecosystem process models for landscape- to regional-scale analysis of the carbon cycle. *Bioscience*, 54:573-584.

Worley, D.P. and G.H. Landis. 1954. The accuracy of height measurements with parallax instruments on 1:12000 photographs. *Photogrammetric Engineering*, 20(1): 823-829.

Wulder, M., K.O. Niemann, and D.G. Goodenough. 2000.Local maximum filtering for the extraction of tree locations andbasal area from high spatial resolution imagery. *Rem. Sens. Envir*. 73:103–114.

Zeide, B., and W.T. Zakrzewski. 1993. Selection of site trees: the combined method and its application. *Can. J. For. Res.* 23:1019–1025.

References from Books:

Goovaerts, P. 1997. Geostatistics for natural resources evaluation. New York, Oxford University Press.

Korpela, I. 2004. Individual tree measurements by means of digital aerial photogrammetry. *Silva Fennica Monographs*, 3:1-93.

References from Other Literature:

Hanson, E.J., D.L. Azuma, and B.A. Hiserote. 2002. Site index equations and mean annual increment equations for Pacific Northwest Research Station Forest Inventory and Analysis Inventories, 1985-2001, Portland, Oregon. USDA Forest Service, Pacific Northwest Research Station, PNW-RN-533.

King, J.E. 1966. Site index curves for Douglas-fir in the Pacific Northwest. *Weyerhaouser For. Pap. 8*. Centralia, WA, USA: Weyerhaouser Company, Weyerhaeuser Forestry Research Center, 49p.